JOURNAL OF MATERIALS SCIENCE 19 (1984) 2643–2650

Craze formation in ABS polymers

R. BRAGLIA
Istituto Guido Donegani S.p.A., Centro Ricerche Novara, Via Fauser, 4, 28100 Novara, Italy

T. CASIRAGHI
Montepolimeri S.p.A., Unità Ricerche Bollate, Via S. Pietro, 50, 20021 Bollate, Italy

The influence of particle morphology, size and distribution and of stressing conditions on craze density and texture has been studied using transmission electron microscopy on three ABS samples. It has been shown that craze density is strongly dependent on particle size and applied stress field. A peculiar texture of crazes is obtained under biaxial loading.

1. Introduction

The well-known phenomenon of stress-whitening of acrylonitrile butadiene styrene (ABS) polymers is unanimously attributed to craze formation and growth [1–10]; the effect is due to the local yielding of the glassy matrix around elastomeric particles because of a high stress concentration, which brings about formation of voids.

The dimensions and structure of crazes are generally studied using transmission electron microscopy (TEM); ultrathin sections are treated with osmium tetroxide (OsO_4) vapour or solutions to enhance the contrast of the rubber particles, as a result of a reaction of OsO_4 with double bonds, and to fill the voids typical of the crazed structure.

Whereas the craze morphology has been studied in great detail by several authors [4–6, 11–15], little is known about the influence of the rubber particle morphology, particle size, size distribution and rubber volume fraction on the craze size and density. Moreover, no investigations have been reported so far on the influence of stressing condition on craze position, size and density. Since it is felt that better knowledge of the effects brought about by the above variables deepens our insight into the crazing phenomenon itself and allows the assessment of the structure–properties relationship for ABS polymers, a TEM study has been undertaken.

2. Experimental details

2.1. Materials

Three injection moulding grade commercial samples of emulsion type ABS (polybutadiene rubber base) were considered. We termed them X, Y and Z. Data on rubber content and mechanical properties are reported in Table I. Nearly isotropic specimens were cut from 3 mm thick plaques prepared by compression moulding of hot-rolled sheets.

2.2. Stressing condition

Specimens were fractured under the stressing conditions reported below.

2.2.1. Tensile impact

This test produces a gradient-less quasi-unixial state of stress on the smallest cross-section of the specimen. The specimen shape, stress profile and image of the broken specimen showing the stress-whitened zone (marked by A) are shown in Figs. 1a and b. Tests were carried out at room temperature (RT) and at an impact speed of 2 m sec^{-1}

2.2.2. Tensile impact on sharply notched specimens

The so-called DEN (double-edge notch) geometry was used; near the tip of the two notches a triaxial state of stress with a very steep gradient is produced. The specimen shape and profile of the stress component along the specimen axis are shown in Fig. 2a. An image of the broken specimen is shown in Fig. 2b (the stress-whitened zone used for the TEM study is marked A). Testing conditions were the same as for tensile impact.

0022–2461/84 $03.00 + .12

TABLE I

Sample	Rubber content (%)	Tensile modulus ($MN\,m^{-2}$)*	Charpy impact ($kJ\,m^{-2}$)		
			$-20°$	$0°$	$23°$
X	17	2400	22	25	24
Y	26	1770	33	36	38
Z	20	2130	17	22	26

*Crosshead speed = $0.1\,m\,sec^{-1}$.

2.2.3. Puncture

The stress field obtained by axial loading of a thin circular plate with an hemispherically shaped punch is practically biaxial. The specimen shape, testing geometry and the associated stress field are shown in Figs. 3a and b.

A photograph of the specimen after testing is shown in Fig. 3c; stress-whitening occurs in the punched part where one can observe the largest variation in the cross-section (Fig. 3d). Tests were carried out at RT and at a testing speed of $0.01\,m\,sec^{-1}$.

2.3. Transmission electron microscopy

Fig. 4 shows how small pyramids were cut out from the fractured specimens. The cutting and microtoming plan was such as to produce ultrathin sections, used for the TEM investigation, parallel to one of the free surfaces of the specimens.

Following the well-known Kato's technique [8–10] pyramids were stained by exposure to OsO_4 vapour at RT for few days. Subsequently, ultrathin sections of about 100 nm were cut using an LKB ultramicrotome with a diamond knife.

All bright-field micrographs were obtained using a 100 kV electron microscope (Philips EM 300).

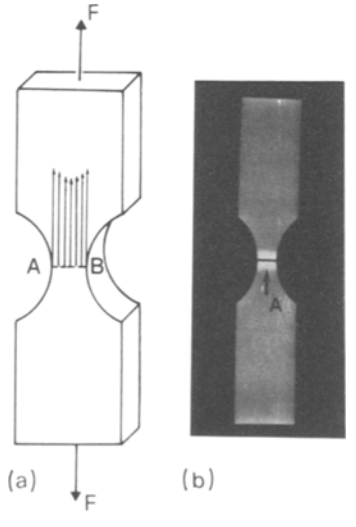

Figure 1 Tensile impact test: (a) schematic view of the specimen and of the associated stress field; (b) view of the broken specimen (the arrow indicates the area whitened by crazing).

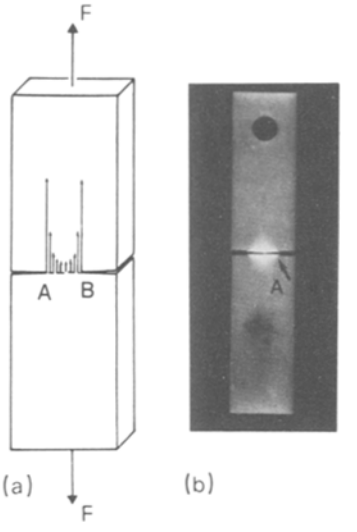

Figure 2 Tensile impact test on sharply notched specimens: (a) schematic view of the specimen and of the associated stress field; (b) view of the broken specimen (the arrow indicates the area whitened by crazing).

3. Results

Before discussing craze morphology it is worth considering the morphology of the ABS samples. Samples X and Y are monomodal with regard to particle size distribution; the distribution is large for both samples and the volumetric centre-line average is at about 350 nm; on the other hand, the particle size distribution of ABS Z is bimodal, but the two distributions are narrow and centred at about 70 and 500 nm (volume average). Moreover, the micrographs show the presence of some very large particles ($\sim 1\,\mu m$ diameter) in samples X and Y. The particle structure of samples X and Y is quite different from that of ABS Z. Particles of ABS X and Y show a large number of rigid phase inclusions which are less evident for ABS Z; in the case of small particles of ABS Z, in particular, inclusions are hard to detect; however, this fact must be critically considered in the light of the instrumental resolving power.

It will be shown below that the mean path of the crazes can be determined by the dimension and number of particles able to initiate crazing.

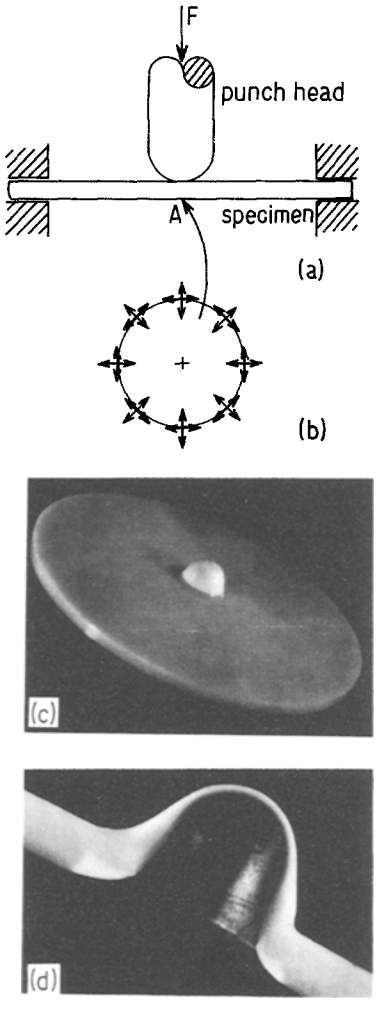

Figure 3 Puncture test: (a) schematic view of the stressing geometry; and (b) of the stress field around point A; (c) view of the large deformation in the centre of the specimen; (d) enlarged section of (c).

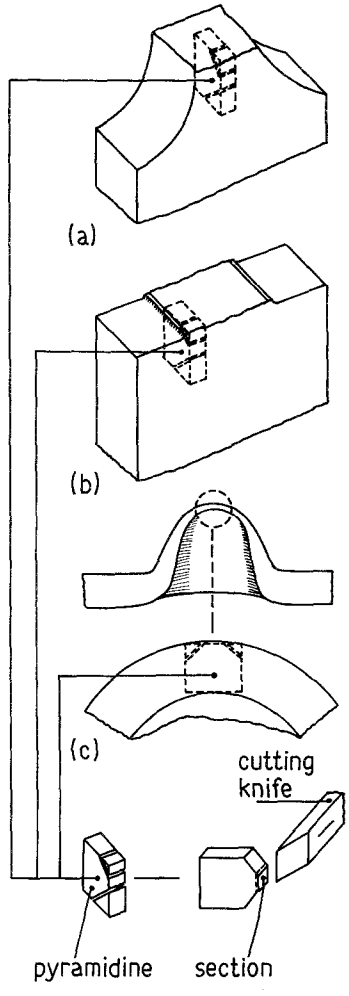

Figure 4 Schematic view of the cutting plane of the TEM specimen from the specimen used and of the cutting direction to obtain thin sections: (a) tensile impact; (b) tensile impact on sharply notched specimens; (c) puncture.

3.1. Tensile impact

Micrographs of ABS X and Y (Figs. 5 and 6) show clearly that particles of all sizes participate in craze formation. Consequently, the craze density is very high: about 70% of the particles participate in craze formation. On the other hand, in the case of ABS Z crazing is generated only by large particles (Fig. 7); in practice, small particles do not contribute to craze initiation but can only affect the paths of growing crazes.

Rubber content, particle size and distribution affect the paths of crazes; the mean path is shortest for sample Y, which has the highest rubber content, is longer for X, which has the same particle size distribution but a lower rubber content, and is longest for ABS Z for which only a fraction of rubber particles is able to generate crazes.

From a mechanical point of view it must be underlined that short craze paths associated with a high craze density facilitate the load relaxation process because of the large number of yielding loci.

As expected in the case of small active particles, crazes initiate from the equator of the particle and lie in a plane perpendicular to the applied stress axis; when large particles are involved in the crazing process it can be observed (Fig. 7) that more than one craze initiates from different points of the particle periphery; therefore, it seems that the "activity" of large particles is higher than that of the smallest ones.

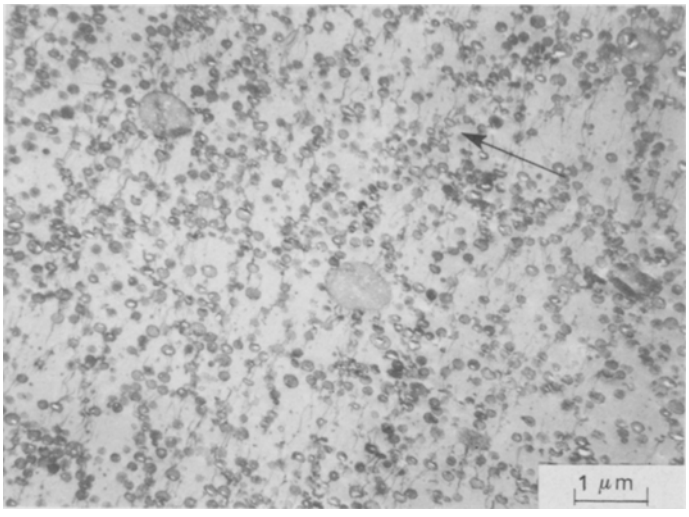

Figure 5 Sample X, tensile impact test; TEM micrograph showing a monomodal distribution, with some very large particles, and a high density of crazes (the arrow indicates the load direction).

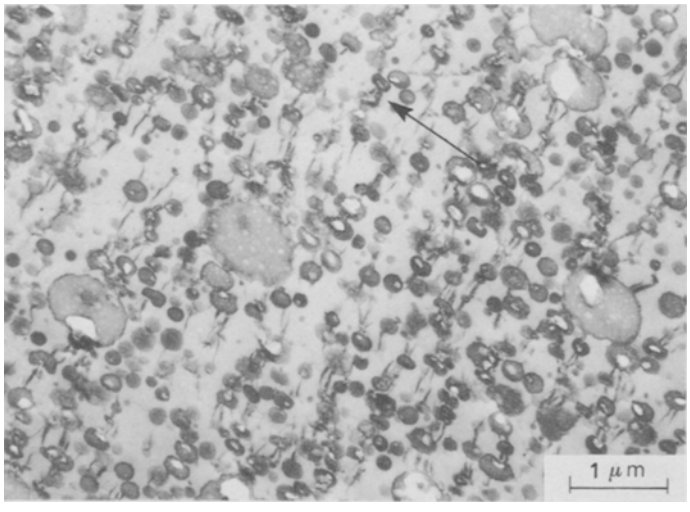

Figure 6 Sample Y, tensile impact test; TEM micrograph showing a monomodal distribution, with some very large particles, and a high density of crazes (the arrow indicates the load direction).

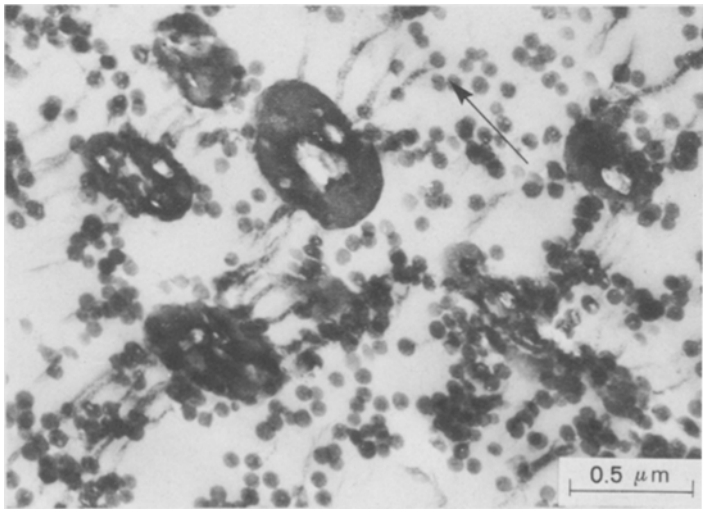

Figure 7 Sample Z, tensile impact test; TEM micrograph showing a bimodal distribution (the arrow indicates the load direction).

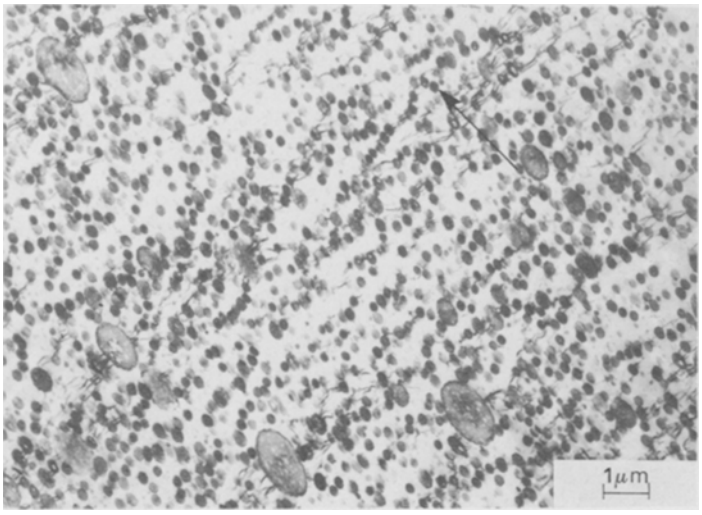

Figure 8 Sample X, tensile impact test on sharply notched specimens (the arrow indicates the load direction).

3.2. Tensile impact on sharply notched specimens

Figs. 8 to 10 show the craze morphology observed for this kind of test. All conclusions drawn for tensile impact similarly hold in this case. In addition, two peculiar features of the morphology of the crazed material are observed: first the large number of particles from which more than one craze initiates; second, the morphology of sample X which appears to be quite different from those of the two other samples: in fact regions of dense crazing alternate with practically unaltered areas. The only explanation which can be put forward is based on the consideration of a very steep stress gradient existing on the neighbourhood of very sharp notches.

3.3. Puncture

Micrographs taken of samples, X, Y and Z are shown in Figs. 11 to 13, respectively. The mean craze path is no longer unidirectional as observed before, but all directions are now possible, as may be expected for a biaxial stress field; crazes initiate not only from the equator of particles but from any diameter.

Craze growth brings about a spun-web morphology which is clearly shown in all micrographs.

Conclusions drawn from the previous experiments about the influence of particle size, size distribution and rubber content also hold in this case.

The low activity of small particles in craze promotion for ABS Z is dramatically shown in

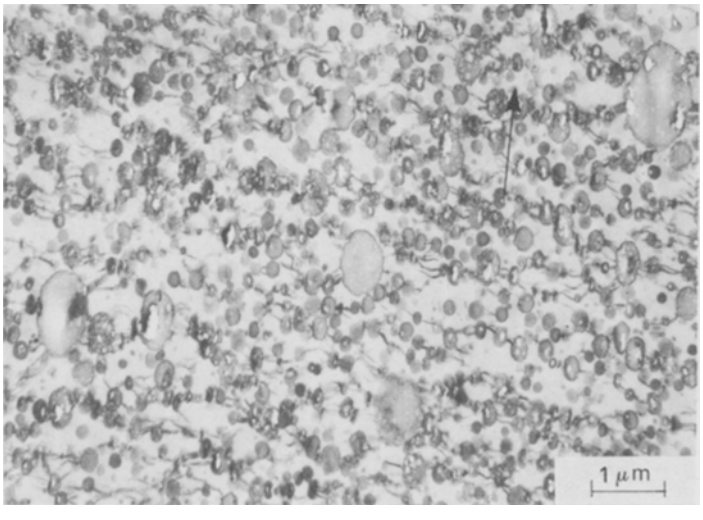

Figure 9 Sample Y, tensile impact test on sharply notched specimens (the arrow indicates and load direction).

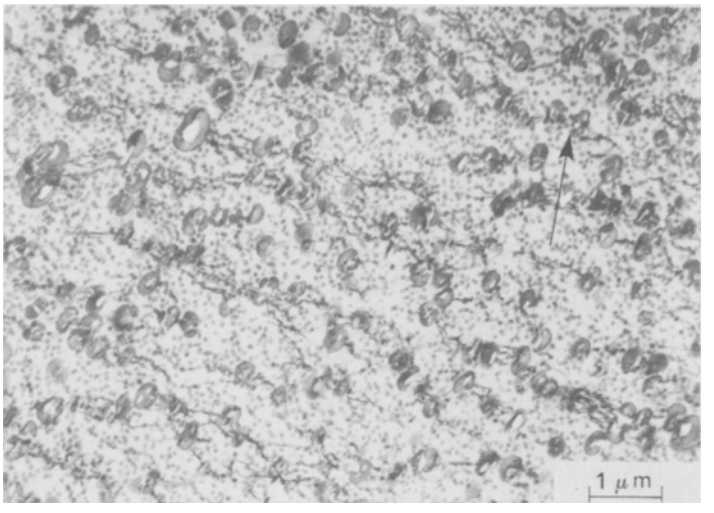

Figure 10 Sample Z, tensile impact test on sharply notched specimens (the arrow indicates the load direction).

Fig. 13, where unperturbed regions filled by small particles are contained in the spun-web texture; nodal points are, in general, located in correspondence to large particles.

Finally, it seems that for all samples the particles of interest in crazing have an irregular shape in comparison to the undeformed ones (see Fig. 12, point A) as a destruction phenomenon has occurred; this is particularly evident from ABS Z (see Fig. 13, point A).

4. Discussion

The TEM study reported here shows that the density and morphology of crazes are dependent on both morphology of the composite and stressing fields. The craze density depends on the rubber content and the size of particles. It appears that a not very sharp monomodal distribution (as for ABS X and Y) with a volume average diameter of 350 nm is favourable for formation of a large number of crazes. As a consequence, not only is energy dissipated in the craze initiation stage but also a large quantity of energy is required for craze propagation. During the latter stage, a flexible network is formed (a highly crazed material can be considered as an expanded structure) which contributes to the energy dissipation. It seems also that the presence of a small number of large particles, able to initiate more than one craze, could play an important role in energy dissipation and in formation of the flexible network, even though the mechanism is not completely clear.

The peculiar behaviour of sample Z indicates that below a critical size the stress field generated

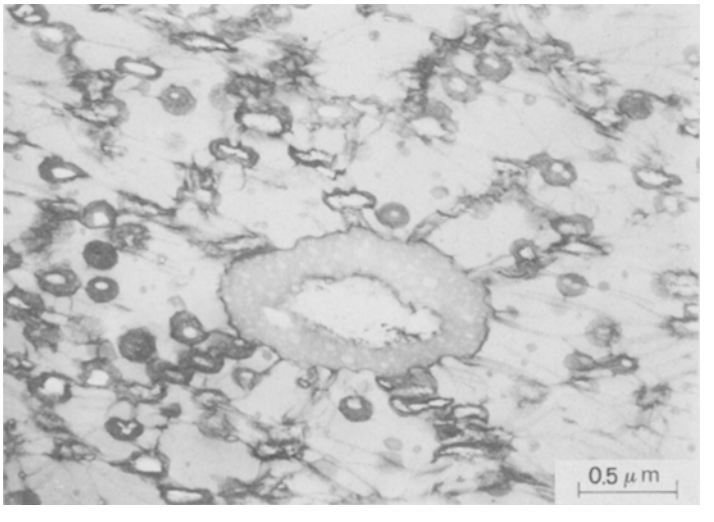

Figure 11 Sample X, puncture test.

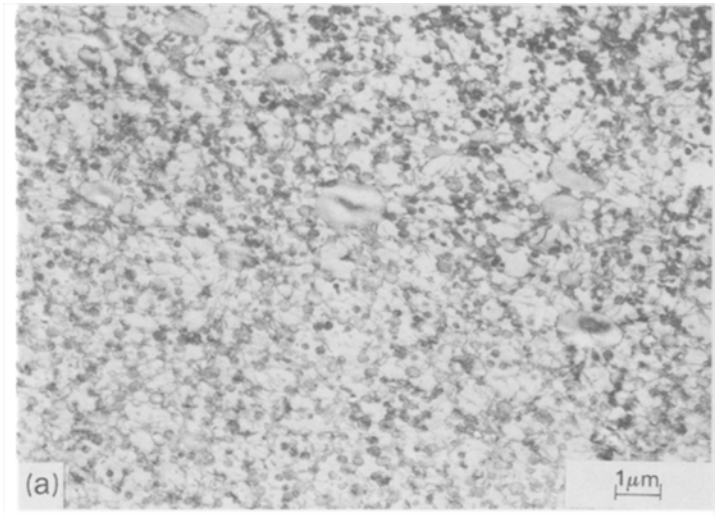

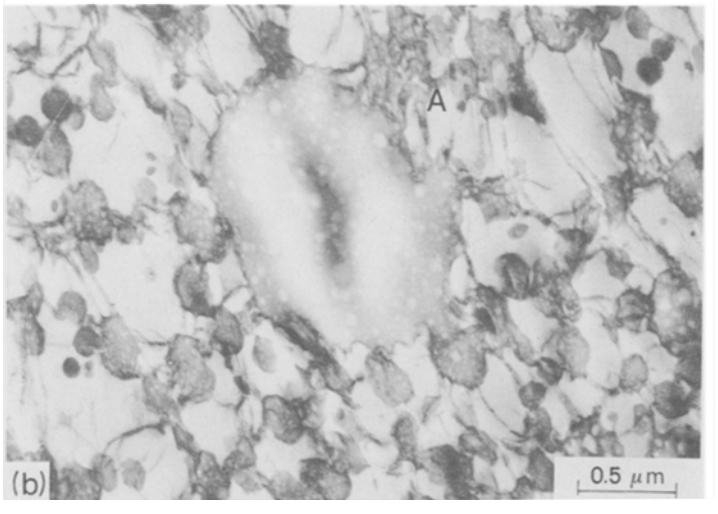

Figure 12 Sample Y, puncture test; the high density of crazing with spun-web morphology is shown in (a); destruction phenomenon at point A is shown in (b).

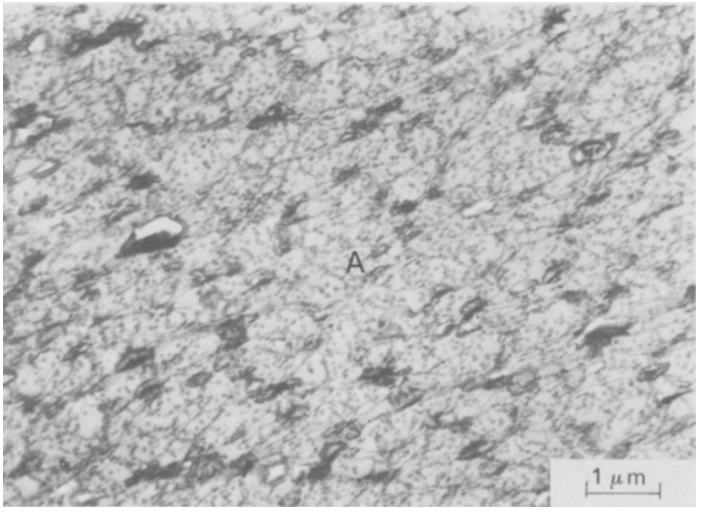

Figure 13 Sample Z, puncture test; point A is an example of destruction phenomenon.

around the particle is insufficient to promote local yielding. As a result, the dissipation efficiency of small particles is low in comparison with that of large particles; from a mechanical point of view it can be concluded that sample Z contains a large fraction of rubber which is active in lowering the modulus of the composite but which is inefficient for increasing the impact strength.

The TEM results agree well with literature data [7, 16] concerning the toughening power of rubber particles as a function of their mean diameter; it is indeed well known that the impact strength of ABS polymers containing small particles is very low. The results appear to hold for each stressing condition considered. As expected on the basis of the applied stress field, this study shows that the morphology of the crazed material is strongly dependent on the stressing conditions.

A peculiar texture of crazes, the hitherto unobserved spun-web morphology, is generated by biaxial loading; the high density of crazing associated with this stressing condition is certainly representative of a high dissipation of energy; moreover, destruction phenomena are observed under this kind of loading. It is emphasized that the results obtained with the puncture test are, at the same time, representative of the very popular falling weight test because of the same stress field. The result reported in a previous paper [17], that the gain in impact strength with respect to the glassy matrix is the highest for biaxial testing, is in good agreement with the present TEM results. Finally, a certain degree of discontinuity in the craze distribution is shown for specimens containing sharp notches. This effect can tentatively be attributed to the sharp notch which brings about a localized stress intensification and to the associated short experience time.

Acknowledgements

Many thanks are due to Dr G. Ajroldi for helpful suggestions and to Mrs G. Agazzini and G. Castiglioni for their contributions in experimental work.

References

1. J. A. SCHMITT and H. KESKKULA, *J. Appl. Polymer Sci.* **3** (1960) 132.
2. C. B. BUCKNALL and R. R. SMITH, *Polymer* **6** (1965) 437.
3. M. MATSUO, *Polymer Eng. Sci.* **9** (1969) 206.
4. C. B. BUCKNALL and I. C. DRINKWATER, *J. Mater. Sci.* 8 (1973) 1800.
5. R. P. KAMBOUR, *Polymer Sci. Makromol. Rev.* **7** (1973) 1.
6. P. J. FENELON and J. R. WILSON, *ACS/A.C. Ser.* **154** (1976) 247.
7. C. B. BUCKNALL, "Toughened Plastics" (Applied Science, London, 1977).
8. K. KATO, *J. Elec. Micr.* **14** (1965) 220.
9. *Idem, Polymer Eng. Sci.* 7 (1967) 38.
10. *Idem, Kolloid Z. Z Polymer* **220** (1967) 24.
11. R. P. KAMBOUR, *Polymer* **5** (1964) 143.
12. *Idem, J. Polymer Sci.* **A2** (1964) 4159.
13. P. BEAHAN, M. BEVIS and D. HULL, *J. Mater. Sci.* 8 (1973) 162.
14. P. BEAHAN, A. THOMAS and M. BEVIS, *J. Mater. Sci.* **11** (1976) 1207.
15. R. W. TRUSS and G. A. CHADWICK, *ibid.* **11** (1976) 1385.
16. L. MORBITZER, D. KRANZ, G. HUMME and K. H. OTT, *J. Appl. Polymer Sci.* **20** (1976) 2691.
17. T. CASIRAGHI, G. CASTIGLIONI and G. AJROLDI, *Plast. Rubb. Process. Appl.* **2** (1982) 353.

Received 28 July
and accepted 29 November 1983